Middle-East Journal of Scientific Research 15 (9): 1255-1263, 2013
ISSN 1990-9233

DOI: 10.5829/idosi.mejsr.2013.15.9.11470

Application of Three Different Calibration-Uncertainty Analysis Methods in a Semi-Distributed Rainfall-Runoff Model Application

[1]Mohsen Pourreza Bilondi, [2]Karim C. Abbaspour and [3]Bijan Ghahraman

[1]Department of Water Engineering, University of Birjand, Birjand, Iran
[2]Swiss Federal Institute for Aquatic Science and Technology, EAWAG,
Ueberlandstrasse 133, P.O. Box 611, CH-8600, Dübendorf, Switzerland
[3]Department of Water Engineering, College of Agriculture,
Ferdowsi Univ. of Mashhad, Mashhad, Iran

Abstract: Often parameters in hydrologic models cannot be measured directly and can only be inferred by a calibration process. This work addresses the application and comparison of three parameter uncertainty methods and their effects on the prediction of streamflow in Qezel Ozan watershed (43,000 km^2) located in northwestern Iran. Methods of Partcle Swarm Optimization (PSO), DiffeRential Evolution Adaptive Metropolis (DREAM) and Sequential Uncertainty Fitting ver. 2 (SUFI2) were used in this study to calibrate a rainfall-runoff model created using the Soil and Water Assessment Tool (SWAT). The calibration and validation results indicated statistically insignificant differences among the three algorithms. The main difference was in their number of runs, where DREAM converged after 36000 runs, PSO after 6000 runs and SUFI2 after 1500 runs. SUFI2 proved to be a very efficient optimization algorithm, while PSO had the largest NS for calibration (0.59) and validation (0.74) periods.

Key words: Uncertainty analysis · SWAT · Differential Evolution Adaptive Metropolis algorithm · PSO · SUFI2

INTRODUCTION

Rainfall-runoff models are widely used in Hydrology to simulate river basin water quality and quantity and play an important role in management of water resources. Hydrologic models such as HSPF (Hydrological simulation program- FORTRAN) [1], SHETRAN [2] and SWAT (Soil and Water Assessment Tool) [3] require many parameters that cannot be measured directly and must only be estimated by calibration against a historical record of measured output data. Due to the problem of non-uniqueness the uncertainty in the model prediction must also be estimated [4]. The major sources of uncertainty are input data, model structure and model parameters [5]. Input uncertainty is often related to imprecise or spatially interpolated measurements of model input and lack of knowledge of initial conditions. Sources of model structural uncertainty include processes not accounted for in the model such as unknown activities in the watershed and model inaccuracy due to over-simplification of the processes considered in the model. Parameter uncertainties arise due to a large number of unknown parameters in distributed models. Furthermore, errors may come from the imprecise measured data used for calibration [6].

Different calibration-uncertainty analysis techniques have different levels of mathematical complexity and data requirements. Topliceanu [7] classified them into two main categories: analytical approaches and approximation approaches. The selection of an appropriate technique to be used depends on the nature of the problem including availability of information, resources constraints, model complexity and type and accuracy of desired results. As most of the models used in hydrology are nonlinear and highly complex, the analytical techniques do not apply because they are rather restrictive in practical applications. Yang *et al*. [6] divided calibration techniques into three main categories: (i) approaches without

Corresponding Author: Mohsen Pourreza Bilondia, Department of Water Engineering, University of Birjand, Birjand, Iran.

rigorous statistical assumptions such as GLUE [8] and SUFI2 [9, 10] (ii) approaches that account for the effect of input errors on the output by an additive error model which introduces temporal correlation of the residuals like autoregressive error models [11,12] and (iii) methods that use improved likelihood functions that explicitly represent input errors and/or model structural error of the underlying hydrological model [6].

Despite the large number of suggested techniques, only a few papers on comparison of different uncertainty analysis techniques are available [6,13,14]. Yang *et al*. [6] compared GLUE, parameter Solution (ParaSol) [15], SUFI2 [10] and MCMC [4,12,16,17] methods in an application to a watershed in China with SWAT model and found that different methods converge to different solutions with more or less the same calibration and validation results. Zhang *et al* [18] also compared five global optimization algorithms (genetic algorithms, shuffled complex evolution, particle swarm optimization, differential evolution and artificial immune system) and showed that particle swarm optimization (PSO) can obtain better parameter solutions than other algorithms given fewer number of model runs (less than 2000).

In this paper we apply a relatively new MCMC procedure entitled DiffeRential Evolution Adaptive Metropolis (DREAM) [19]. We applied DREAM to a rainfall-runoff model built using SWAT and compare the results with PSO [20] and SUFI2, where the latter is reported by Yang *et al*. [6] to need a smaller number of model runs in comparison with other methods. As Yang *et al*. [6] explained there are various difficulties in comparing uncertainty analysis techniques. In this paper, we compare the final calibration and validation statistics (e.g. R^2, NS, MSE) and the uncertainty statistics suggested by Abbaspour et al. (2004, 2007) [9,10] (e.g. *R-factor* and *P-factor*), which compare the observation signal with the 95% prediction uncertainty band.

MATERIALS AND METHODS

Description of the Study Area: This study was conducted in a section of Qezel Ozan watershed (Fig 1) with a drainage area of 43000 km^2 located in northwestern Iran. The river originates from the mountains of Kurdistan (from South to north) and discharges to the Caspian Sea. The average annual precipitation, average daily minimum and maximum temperatures respectively are 319 mm, 5.5°C and 20.5 °C. According to De Martonne formula this region has a climate zone of arid to semi-arid. Average

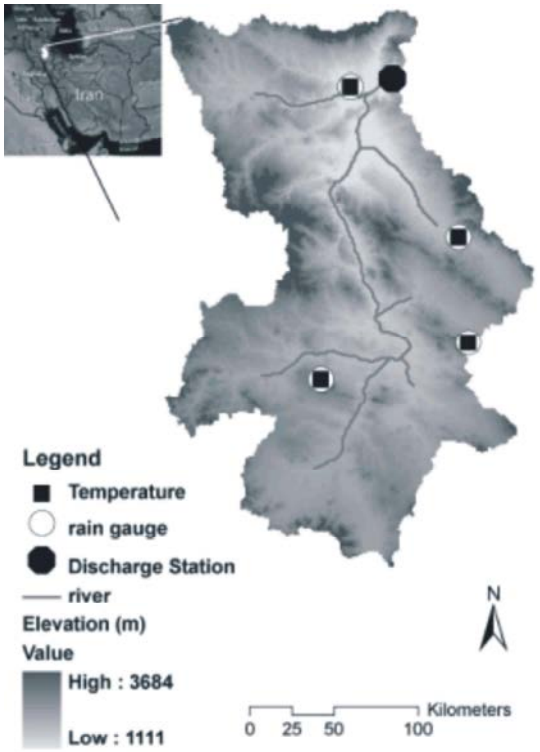

Fig. 1: Location of study site as well hydrometric stations, rain and temperature stations

daily discharge for over a 30-years period (1975-2004) at the basin outlet is 60 m^3s^{-1} and varies irregularly between 790 m^3 s^{-1} during flood season to 17 m^3 s^{-1} in the dry season. Grassland covers more than 85% of the area. Figure 1 shows the location of the watershed along with temperature gauge, rain gauge and discharge stations.

Hydrological Model (SWAT): The Soil and Water Assessment Tool (SWAT) [3] was used in the current study. We chose SWAT because of its availability and user-friendliness in handling input data. Swat is continuous time, spatially distributed simulator of water, sediment, nutrients and pesticides transport at a catchment scale. In SWAT, a watershed is divided into a number of sub-basins based on given digital elevation model (DEM) and then a sub-basin is allowed to be divided into a number of unique hydrologic response units (HRU) based on variability in soil, slope and land use characteristics.

The hydrologic model is based on the water balance for the four storage volumes snow, soil profile (0-2 m), shallow aquifer (2-20 m) and deep aquifer (>20 m). The simulated processes include surface runoff, infiltration, evaporation, plant water uptake, lateral flow and

Table 1: The 9 most sensitive parameters for uncertainty analysis and their initial ranges

		1Initial range	
Aggregate parameters	Description	Min	Max
r__SOL_BD(1).sol	Soil bulk density (g cm^{-3})	-0.8	0.8
r__SOL_AWC(1).sol	Soil available water storage capacity (mm H_2O/mm soil)	-0.9	0.9
v__ALPHA_BNK.rte	Base flow alpha factor for bank storage (days)	0	1
v__CH_K2.rte	Effective hydraulic conductivity in the main channel (mm h^{-1})	0	150
v__CH_N2.rte	Manning's n value for main channel	0	0.3
v__ESCO.hru	Soil evaporation compensation factor	0.01	1
r__CN2.mgt	SCS runoff curve number for moisture condition II	-0.7	0.7
r__HRU_SLP.hru	Average slope steepness (m/m)	-0.8	0.8
v__CANMX.hru	Maximum canopy index	0	100

percolation to shallow and deep aquifers. Depending on data availability, the potential evapotranspiration (PET) can be computed using different methods. In this study, potential evapotranspiration (PET) was simulated using the Hargreaves method [21] Based on the PET and additional soil and landuse parameters, the actual plant transpiration and the actual soil evaporation are estimated separately. The surface runoff from daily rainfall amounts is modelled using a modification of the SCS curve number method [22] taking into account landuse, soil type and antecedent soil moisture. Based on the literature and one factor-at-a-time sensitivity analysis we selected 9 parameters for model calibration (Table 1).

SUFI2 Procedure: SUFI2 [10] is a tool for sensitivity analysis, multi-site calibration and uncertainty analysis. It is capable of analyzing a large number of parameters and measured data from many gauging stations simultaneously. In SUFI-2, parameter uncertainty is described by a multivariate uniform distribution in a parameter hypercube, while the output uncertainty is quantified by 95PPU calculated at the 2.5% and 97.5% levels of the cumulative distribution function of the output variables. Latin hypercube sampling is used to draw independent parameter sets [10] SUFI2 is linked to SWAT (in the SWAT-CUP software; Abbaspour, 2011) [23] through an interface that also includes the programs Generalized Likelihood Uncertainty Estimation (GLUE) [8], PSO, Parameter Solution (ParaSol) [15] and a Monte Carlo Markov Chain (MCMC) [17] algorithm. A full detailed description of SUFI2 is presented by Abbaspour *et al*. [9, 10].

Particle Swarm Optimization: Particle swarm optimization (PSO) is a population based stochastic optimization technique developed by Eberhart and Kennedy [20], inspired by social behavior of bird flocking or fish schooling [23]. Many researcher in water science successfully have applied it as a search engine to optimize parameters of the models [24-26]. PSO shares many similarities with evolutionary computation techniques such as Genetic Algorithms (GA). The basic PSO algorithm consists of three steps: (i) generate the positions of particles (coordinate in the parameter space) and their velocities ('flying' direction and speed); (ii) update the velocity of each particle using the information from the best solution it has achieved so far (personal best) and another solution with the best fitness value that has been obtained so far by all the particles in the population (global best); (iii) finally, the new position of each particle is calculated by adding the updated velocity to the current position [18].

Markov chain Monte Carlo (MCMC): We took advantage of a novel Markov chain Monte Carlo (MCMC) sampler, entitled differential evolution adaptive Metropolis (DREAM). This approach is known as the latest MCMC schemes developed by Vrugt *et al*. [19] and is applicable to complex, multi-modal, search problems and on a wide range of model calibration and uncertainty studies to estimate optimal parameter values and their underlying posterior probability density function [27-31]. Vrugt *et al*. [19] showed that DREAM works really well as compared to the other existing MCMC schemes.

The DREAM sampling scheme in fact is an adaptation of the Shuffled Complex Evolution Metropolis (SCEM-UA) global optimisation algorithm [17].

In the DREAM algorithm differential evolution as a genetic algorithm is used for population evolution. Within this technique a preset number (N) of Markov Chains (a chain refers to a vector containing one parameter realization) are simultaneously run in parallel. The chains are initialized by latin hypercube sampling the parameter space using uniform distribution. These chains form a population, conveniently stored as a N × d matrix X, with d the dimension of the parameter space. For each chain, i

$i \in \{1, 2,... N\}$, a candidate point z_i (vector) is generated by taking a fixed multiple of the difference between randomly chosen pairs of chains (without replacement) of X_{-i} (X without x_i) [32] :

$$z_i = x_i + (1 + e)\gamma(\delta, d_{eff})\left[\sum_{j=1}^{\delta} x_{r_1(j)} - \sum_{n=1}^{\delta} x_{r_2(n)}\right] + \varepsilon \quad (1)$$

Where δ signifies the number of pairs used to generate the proposal, γ is a jumprate and $r_1(j)$, $r_2(n) \in \{1, 2,...,N\}$ but $r_1(j) \neq r_2(n) \neq i$. The value of e is drawn from $U_d(-b, b)$ with $|b| < 1$ and $\varepsilon \sim N_d(0, b^*)$ is a white noise term with b* small compared to the width of the target distribution. The Metropolis ratio is used to decide whether to accept the candidate point or not. If accepted, the chain moves from x_i to z_i, otherwise the location of the chain remains unchanged. From the guidelines of γ in Random Walk Metropolis (RWM), a good choice of $\gamma = 2.38/\sqrt{2\delta.d_{eff}}$, where d_{eff} denotes the number of dimensions that will be updated. With this approach, a Markov chain is obtained, the stationary distribution of which is the posterior distribution. After a so-called burn-in period, the convergence of a DREAM run can be monitored with the $\hat{R}$ -statistic of Gelman and Rubin [33], which compares the variance within and between the chains. A value of $\hat{R}$ smaller than 1.2 for each parameter ($\hat{R}_k < 1.2$, k=1, 2,..., d) diagnoses convergence to a limiting distribution. The samples generated after convergence can be used to summarize the posterior distribution and communicate parameter and model predictive uncertainty. The number of steps in each chain required to reach stationarity (convergence) is commonly called "burn-in" and these samples are removed from the analysis [28] A detailed description of DREAM appears in Vrugt *et al*. [32].

DREAM is actually available now as a package in R developed by Guillaume and Andrews [34] (from R-forge) and in this study it was linked with SWAT.

Criteria for the Comparison: We use the commonly used Nash-Sutcliffe (NS) as objective function. Two indices are used to quantify the goodness of calibration/uncertainty performance [9, 10] the *P-factor*, which is the percentage of data bracketed by the 95% prediction uncertainty band (95PPU) (maximum value 100%) and the *R-factor*, which is the average width of the band divided by the standard deviation of the corresponding measured variable (minimum 0).

RESULT AND DISCUSSION

Results of SUFI2: SUFI2 implementation is convenient and easy. The modeler, however, should check a set of suggested posterior parameters to be prepared for next iterations. Parallelizing the runs in SUFI2 [35] has substantially decreased the calibration time of SUFI2 in SWAT-CUP. SUFI2 is an iterative procedure. In this study we performed three iterations of 500 simulations each. The calibration period was 9 years (1993-2001) with three years used as warm-up period. In the third iteration, the 95PPU brackets 48% of the observations and r-factor equals 0.51. For the validation period (1990-1992) the *P-factor* and *R-factor* were, respectively, 0.31 and 0.53. Figure 2 describes the 95PPU (light grey area) in both calibration and validation periods as well as the observation points. The solid line is the best simulation based on the run with the largest NS. Same periods for calibration and validation like SUFI2 are considered for two other methods.

Posterior distributions in SUFI2 are aways independent and mostly uniformly distributed and expressed as narrowed parameter ranges. Also, there are no correlations between different parameters (all R^2s less than 0.25), as samples are taken randomly using Latin hypercube sampling.

Result of PSO: Like SUFI2, PSO also is linked to SWAT (in the SWAT-CUP software, Abbaspour, 2011) and its implementation is easy. We carried out totally 6000 simulation runs (e.g. 6 iterations with 1000 simulations). The 95PPU brackets 66% of the observations and r-factor equals 0.73. For the validation period the *R-factor* and *P-factor* were, respectively, 0.61 and 0.83. Figure 3 describes the 95PPU (light grey area) in both calibration and validation periods as well as the observation points. The solid line is the best simulation based on the run with the largest NS.

Marginal posterior distribution just in connection with v__ALPHA_BNK.rte parameter is illustrated in Figure 4. Remaining parameters have irregular posterior distributions and are not shown.

Result of DREAM: We used a number of chains or population size of N = 2d, d as the number of parameters, with a maximum total of 36,000 model evaluations for SWAT. Samples with NS more than 0.4 (like SUFI2) in each of the 18 chains were selected as the behavioral samples and 95PPU, *P-factor* and *R-factor* are based on the results that adopted from behavioral parameters.

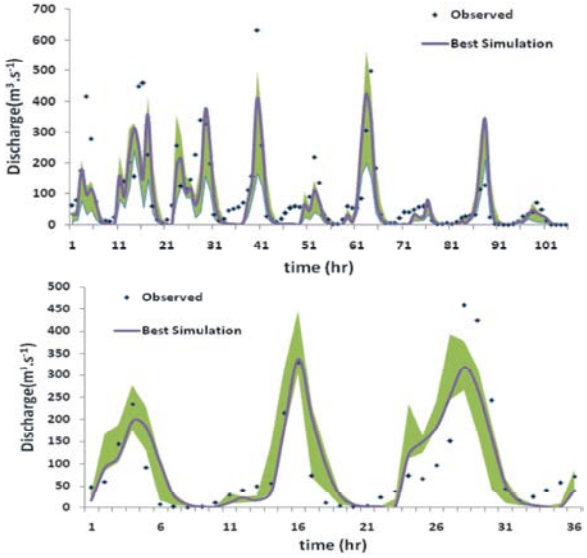

Fig. 2: 95PPUs derived by SUFI2 (dark gray area) during the calibration period (top) and validation period (bottom). The dots correspond to the observed discharge at the basin outlet, while the solid line represents the best simulation obtained by SUFI2.

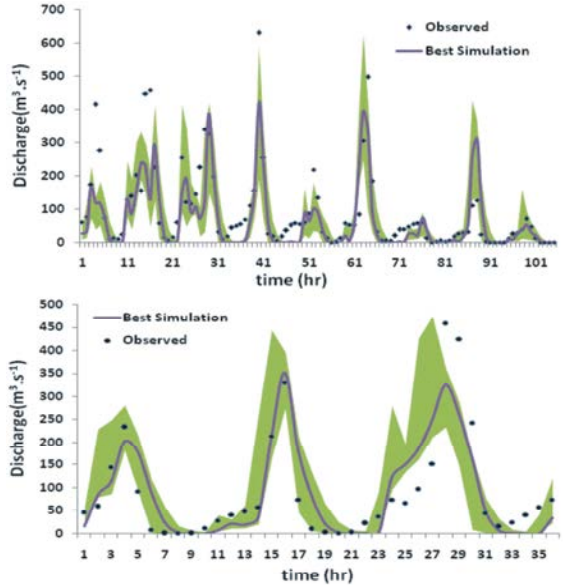

Fig. 3: 95PPUs derived by PSO (dark gray area) during the calibration period (top) and validation period (bottom). The dots correspond to the observed discharge at the basin outlet, while the solid line represents the best simulation obtained by PSO.

Figure 5 presents the 95PPU with light grey area in both calibration and validation periods. The results for both calibration and validation periods show observational discharge values bracketed partly well within 95PPU with

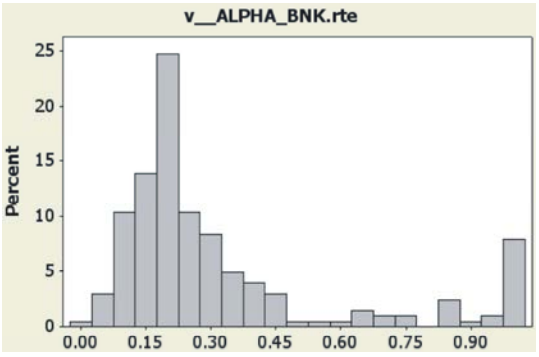

Fig. 4: Histogram approximating the marginal posterior distributions of aggregate SWAT behavioral parameter conditioning with PSO

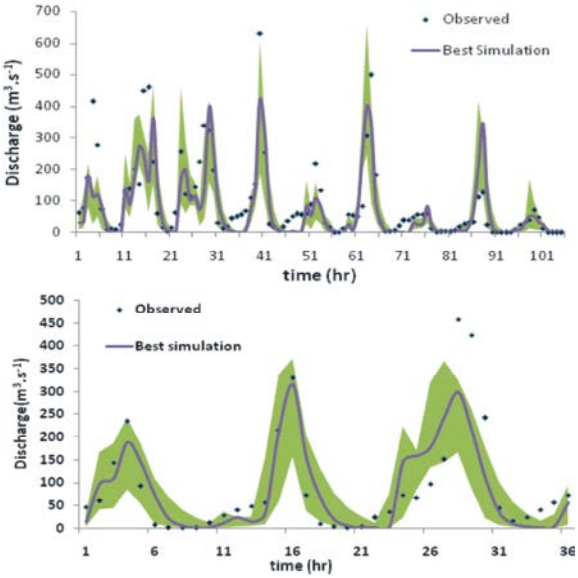

Fig. 5: 95PPUs derived by DREAM (dark gray area) during the calibration period (top) and validation period (bottom). The dots correspond to the observed discharge at the basin outlet, while the solid line represents the best simulation obtained by DREAM.

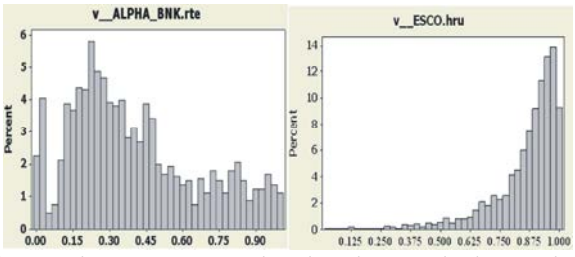

Fig. 6: Histograms approximating the marginal posterior distributions of aggregate SWAT behavioral parameters conditioning with Bayesian MCMC - DREAM.

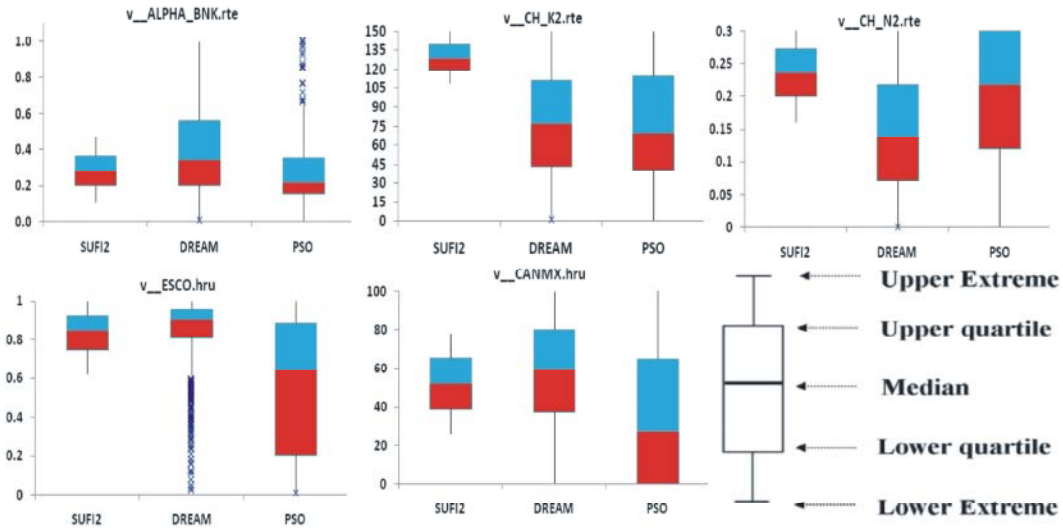

Fig. 7: Box plots of parameters (on a ratio scale) uncertainty range for SUFI2, DREAM and PSO

Table 2: Measures values for three uncertainty methods for parameters on a ratio scale

		Parameters				
Method	Measure	v__ALPHA_BNK	V__CH_K2	v__CH_N2	V__ESCO	v__CANMX
SUFI2	Mean	0.28	129.25	0.24	0.84	52.15
	SD	0.1	11.7	0.04	0.1	15.22
	CV	0.34	0.09	0.18	0.12	0.29
PSO	Mean	0.33	76.12	0.20	0.55	36.59
	SD	0.27	46.53	0.10	0.38	36.47
	CV	0.82	0.61	0.52	0.69	1.00
DREAM	Mean	0.4	77.03	0.14	0.86	57.41
	SD	0.26	41.23	0.09	0.15	27.1
	CV	0.65	0.54	0.6	0.18	0.47

Table 3: Comparison of some measures of performance for both SUFI2 and DREAM in calibration and validation periods

		Best simulation						
Period	Method	R^2	NS	MSE	P-factor	R-Factor	Number of simulation	Number of Behavioral Simulations
Calibration	DREAM	0.61	0.59	6014	0.63	0.67	36000	1599
	SUFI2	0.59	0.57	6311	0.48	0.51	1500	351
	PSO	0.62	0.59	5980	0.66	0.73	6000	202
Validation	DREAM	0.69	0.69	4118	0.53	0.84	7200	-
	SUFI2	0.71	0.71	3768	0.31	0.53	500	-
	PSO	0.74	0.74	3419	0.61	0.83	202	-

P-factor 0.63 and 0.67, respectively for the calibration period. For the validation, *R-factor* was 0.53 and *P-factor* equaled 0.84.

Because of the large number of evaluations in DREAM (36000 vs. 1500 in SUFI2), it can explores the parameter space in more detail and the marginal posterior pdfs can be inferred for some sensitive parameters. Posterior distributions of these individual parameters are well defined and occupy only a relatively small region interior to the uniform prior distributions.

Posterior distributions in connection with two parameters (v__ALPHA_BNK.rte and v__ESCO.hru) are illustrated in Figure 6. Concerning posterior distribution of v__ALPHA_BNK.rte parameter, it shows some similarity with its distribution in PSO (figure 4). Remaining parameters have irregular posterior distributions and are not shown.

The correlations between all parameters in all methods are small and therefore there are no significant correlations.

Comparison the Results: Table 2 lists the mean, standard deviation and coefficient of variation (CV) identified for five most sensitive parameters on a ratio scale which can only take non-negative values. CV is defined as the ratio of the standard deviation to the mean of values. From that table it is resulted that SUFI2 has smallest CVs between two other methods for all five ratio scale parameters.

We get the same results by box-plots for all five ratio scale parameters (also called box and whisker plots) in Figure 7. The line across the box represents the median, whereas the bottom and top of the box show the location of the first and third quartiles ($Q1$ and $Q3$). The whiskers are the lines that extend from the bottom and top of the box to the lowest and highest observations inside the region defined by $Q1 - 1.5(Q3 - Q1)$ and $Q3 + 1.5(Q3 - Q1)$. Individual points with values outside these limits are plotted with asterisks. Box-plot provides a visual comparison of the uncertainty methods in connection with different parameters. As seen for these 5 parameters, SUFI2 box-plots, show small spread around the median (small range of variability and fewer parameter uncertainties) thus revealing the effectiveness and efficiency of SUFI2 as compare to DREAM and PSO. Only the ESCO parameter has as spread around the median in DREAM method which this matter also understandable form table 2 that shows the closeness of their CVs (0.12 compared to 0.18). Since sensitive parameters with smaller CVs show very small range of uncertainty compared to less sensitive parameters, it can be used to specify most sensitive parameters.

Finally, a summary comparison between the three uncertainty methods is provided in Table 3. As seen, *P-factor* for calibration period in DREAM and PSO is larger than SUFI2, but this is because the *R-factor* in SUFI2 is narrower. In validation, PSO with smaller simulation runs than DREAM slightly has better results than it. But from best simulation perspective, PSO results have largest R^2 and NS and smallest MSE among three methods in both periods.

CONCLUSION

As Yang *et al* [6] concluded that SUFI2 technique could be run with the smallest number of model runs to achieve good prediction uncertainty ranges in the sense of a reasonable coverage of data points by the prediction uncertainty bands. This characteristic is very important for computationally demanding models.

In spite of the larger number of simulation in DREAM rather than PSO and SUFI2, it can not provide results better than other, except that two marginal posterior distribution parameters can be obtained from DREAM. In case of v__ALPHA_BNK.rte parameter, PSO also has a posterior distribution some like with that parameter in DREAM. In respect to performance of their best estimates, PSO results have largest R^2 and NS and smallest MSE among three methods in both periods.

In according to CV values, it can be resulted that three parameters of V_CH_K2, V_CH_N2 and V_ESCO in most cases have smallest CV values and then are specified as most sensitive parameters.

ACKNOWLEDGMENTS

Authors would like to thank Dr. John Joseph who helped us to implement SWAT with DREAM package in R. We also would like to have special thanks for Dr. Jasper Vrugt for his useful comments.

REFERENCES

1. Bicknell, B.R., J. Imhoff, J. Kittle, T. Jobes and A.S. Donigian, 2000. Hydrological Simulation Program - Fortran User's Manual. Release 12, US EPA.

2. Ewen, J., G. Parkin and P.E. O'Connell, 2000. SHETRAN: Distributed River Basin Flow and Transport Modeling System. J. Hydrol. Eng., 5: 250-258.
3. Arnold, J.G., R. Srinivasan, R.S. Muttiah and J.R. Williams, 1998. Large area hydrologic modeling and assessment part i: model development1. Jawra Journal of the American Water Resources Association, 34: 73-89.
4. Kuczera, G. and E. Parent, 1998. Monte Carlo assessment of parameter uncertainty in conceptual catchment models: the Metropolis algorithm. Journal of Hydrology, 211(1-4): 69-85.
5. Refsgaard, J.C., J.P. Van der Sluijs, J. Brown and P. Van der Keur, 2006. A framework for dealing with uncertainty due to model structure error. Adv Water Resour, 29: 1586-1597.
6. Yang, J., P. Reichert, K.C. Abbaspour, J. Xia and H. Yang, 2008. Comparing uncertainty analysis techniques for a SWAT application to the Chaohe Basin in China. J. Hydrol., 358: 1-23.

7. Topliceanu, L., 2007. Water resources engineering-Analysis of uncertainty. Romanian Technical Sciences Academy, 1: 295-300.
8. Beven, K. and A. Binley, 1992. The Future of Distributed Models-Model Calibration and Uncertainty Prediction. Hydrol Process, 6: 279-298.
9. Abbaspour, K.C., C.A. Johnson and M.T. Van Genuchten, 2004. Estimating uncertain flow and transport parameters using a sequential uncertainty fitting procedure. Vadose Zone J., 3: 1340-1352.
10. Abbaspour, K.C., J. Yang, I. Maximov, R. Siber, K. Bogner, J. Mieleitner, J. Zobrist and R. Srinivasan, 2007. Modelling hydrology and water quality in the pre-alpine/alpine Thur watershed using SWAT. J Hydrol, 333: 413-430.
11. Campbell, E.P. and B.C. Bates, 2001. Regionalization of rainfall-runoff model parameters using Markov chain Monte Carlo samples. Water Resour Res., 37: 731-739.
12. Yang, J., P. Reichert, K.C. Abbaspour and H. Yang, 2007. Hydrological modelling of the chaohe basin in china: Statistical model formulation and Bayesian inference. J. Hydrol., 340: 167-182.
13. Makowski, D., D. Wallach and M. Tremblay, 2002. Using a Bayesian approach to parameter estimation; comparison of the GLUE and MCMC methods. Agronomie, 22: 191-203.
14. Mantovan, P. and E. Todini, 2006. Hydrological forecasting uncertainty assessment: Incoherence of the GLUE methodology. J. Hydrol., 330: 368-381.
15. Van Griensven, A. and T. Meixner, 2006. Methods to quantify and identify the sources of uncertainty for river basin water quality models. Water Sci. Technol., 53: 51-59.
16. Marshall, L., D. Nott and A. Sharma 2004. A comparative study of Markov chain Monte Carlo methods for conceptual rainfall-runoff modeling. Water Resources Research, 40, W02501, doi:10.1029/2003WR002378. M.D. McKay, R.J. Beckman, W. Conover,
17. Vrugt, J.A., H.V. Gupta, W. Bouten and S. Sorooshian, 2003. A Shuffled Complex Evolution Metropolis algorithm for optimization and uncertainty assessment of hydrologic model parameters. Water Resour. Res., 39: 1201.
18. Zhang, X., R. Srinivasan, K. Zhao and M. Van Liew, 2008. Evaluation of global optimization algorithms for parameter calibration of a computationally intensive hydrologic model. Hydrol. Process, 23: 430-441.
19. Vrugt, J.A., C.J.F.T. Braak, C.G.H. Diks, B.A. Robinson, J.M. Hyman and D. Higdon, 2009b. Accelerating Markov chain Monte Carlo simulation by differential evolution with self-adaptive randomized subspace sampling. International Journal of Nonlinear Sciences and Numerical Simulation, 10: 273-290.
20. Eberhart, R.C. and J. Kennedy, 1995. A new optimizer using particle swarm theory. Proceedings of the sixth international symposium on micro machine and human science pp: 39-43. IEEE service center, Piscataway, NJ, Nagoya, Japan.
21. Hargreaves, G.L., G.H. Hargreaves and J.P. Riley, 1985. Agricultural benefits for Senegal River Basin. Journal of Irrigation and Drainage Engineering, 111: 113-124.
22. USDA Soil Conservation Service. 1972. National Engineering Handbook Section 4 Hydrology, Chapter, pp: 4-10.
23. Abbaspour, K.C., 2011. Swat-Cup4 SWAT Calibration and Uncertainty Programs Manual Version 4, Department of Systems Analysis, Integrated Assessment and Modelling SIAM, Eawag. Swiss Federal Institute of Aquatic Science and Technology, Duebendorf, Switzerland.
24. Reddy, M.J. and D. Nagesh Kumar, 2007. Multi-objective particle swarm optimization for generating optimal trade-offs in reservoir operation. Hydrol Process, 21: 2897- 2909.
25. Gaur, S., D. Mimoun and D. Graillot, 2011. Advantages of the analytic element method for the solution of groundwater management problems. Hydrol Process, 25: 3426- 3436.
26. Lu, H., Z. Yu, R. Horton, Y. Zhu, Z. Wang, Z. Hao and L. Xiang, 2011. Multi-scale assimilation of root zone soil water predictions. Hydrol Process, 25: 3158-3172.
27. Vrugt, J.A., C.J.F. ter Braak, M.P. Clark, J.M. Hyman and B.A. Robinson, 2008. Treatment of input uncertainty in hydrologic modeling: Doing hydrology backward with Markov chain Monte Carlo simulation. Water Resour. Res., 44: W00B09.
28. Dekker, S.C., J.A. Vrugt and R.J. Elkington, 2010. Significant variation in vegetation characteristics and dynamics from ecohydrological optimality of net carbon profit. Ecohydrology, na-na.
29. Laloy, E., D. Fasbender and C.L. Bielders, 2010a. Parameter optimization and uncertainty analysis for plot-scale continuous modeling of runoff using a formal Bayesian approach. J. Hydrol., 380: 82-93.

30. Laloy, E., M. Weynants, C.L. Bielders, M. Vanclooster and M. Javaux, 2010b. How efficient are one-dimensional models to reproduce the hydrodynamic behavior of structured soils subjected to multi-step outflow experiments? J. Hydrol., 393: 37-52.
31. Scharnagl, B., J.A. Vrugt, H. Vereecken and M. Herbst, 2010. Information content of incubation experiments for inverse estimation of pools in the Rothamsted carbon model a Bayesian perspective. Biogeosciences, 7: 763-776.
32. Vrugt, J., C. ter Braak, H. Gupta and B. Robinson, 2009a. Equifinality of formal DREAM and informal GLUE Bayesian approaches in hydrologic modeling? Stoch Env Res Risk A, 23: 1011-1026.
33. Gelman, A. and D.B. Rubin, 1992. Inference from iterative simulation using multiple sequences, Stat. Sci., 7: 457-472.
34. Guillaume, J. and F. Andrews, 2010. https://r-forge.r-project.org/scm/viewvc.php /pkg/DESCRIPTION ? view=markup&revision=33&root=dream&pathrev=33
35. Rouholahnejad, E., K.C. Abbaspour, M. Vejdani, R. Srinivasan, R. Schulin and A. Lehmann, 2011. Parallelizing SWAT calibration in Windows using the SUFI2 program. Environmental Modelling and Software.